JGR Biogeosciences

RESEARCH ARTICLE
10.1029/2023JG007750

# Net Primary Production of Ecoregions Across North America in Response to Drought and Wildfires From 2015 to 2022

**Christopher Potter**[1], **Stephanie Pass**[2], **and Rachel Ulrich**[3,4]

[1]NASA Ames Research Center, Moffett Field, CA, USA, [2]University of California, Berkeley, CA, USA, [3]Montana State University, Bozeman, MT, USA, [4]Los Alamos National Laboratory, Los Alamos, NM, USA

**Key Points:**

- Our main finding is that extensive and extreme drought across North America in 2020 and 2021 depressed plant production by 10%–20% compared to the previous 5 years
- Warmer, drier climate conditions are leading to lower tree regeneration after wildfires in the past decade, compared to the decades of the 1980s and 1990s
- Trends in NPP in large wildfires of 2012–2014 indicated that extreme drought periods can depress NPP recovery even 5–7 years post-fire

**Supporting Information:**

Supporting Information may be found in the online version of this article.

**Correspondence to:**

C. Potter,
chris.potter@nasa.gov

**Citation:**

Potter, C., Pass, S., & Ulrich, R. (2024). Net primary production of ecoregions across North America in response to drought and wildfires from 2015 to 2022. *Journal of Geophysical Research: Biogeosciences*, *129*, e2023JG007750. https://doi.org/10.1029/2023JG007750

Received 15 AUG 2023
Accepted 17 MAR 2024

**Author Contributions:**

**Conceptualization:** Christopher Potter
**Data curation:** Christopher Potter, Stephanie Pass
**Formal analysis:** Christopher Potter, Stephanie Pass
**Funding acquisition:** Christopher Potter
**Investigation:** Christopher Potter
**Methodology:** Christopher Potter, Rachel Ulrich
**Project administration:** Christopher Potter
**Resources:** Christopher Potter
**Software:** Christopher Potter, Stephanie Pass, Rachel Ulrich



**Abstract** Ecosystem models are valuable tools to make climate-related assessments of change when ground-based measurements of water and carbon fluxes are not adequate to realistically capture regional variability. The Carnegie-Ames-Stanford Approach (CASA) is one such model based on satellite observations of monthly vegetation cover to estimate net primary production (NPP) of terrestrial ecosystems. CASA model predictions from 2015 to 2022 revealed several notable high and low periods in growing season NPP totals in certain biomes. Both Temperate Broadleaf and Boreal Forest production shifted from relatively high average NPP values in 2015 through 2019 to lower levels in 2020, typically representing a loss of 10%–14% of growing season NPP flux. This rapid decline in growing season NPP from 2019 to 2020–2021 was also estimated for the Temperate Grasslands and Savanna, Temperate Conifer Forest, and Tundra biomes. In contrast to the climate patterns in the temperate biomes that developed into severe widespread drought in 2020 and 2021 due to low precipitation totals and extreme hot temperatures, growing season NPP in the Tundra biome was depressed in these same years by colder temperature induced drought conditions at the high latitudes of North America. Drought severity classes were closely associated with different levels of decline in NPP in most biomes. Trends in NPP in areas of the largest wildfires in North America that burned between 2012 and 2021 were examined to assess recovery of vegetation and the resiliency of ecosystems during extreme drought periods.

**Plain Language Summary** Annual growth of terrestrial plant cover, also known as net primary production (NPP), must be maintained and managed by societies worldwide to meet their essential needs for food and fiber. A model of global NPP that uses monthly satellite images as inputs predicted that extreme drought in the years 2020 and 2021 across North America, caused by greatly diminished precipitation totals and hot temperatures, depressed continental plant production by 10%–20% compared to the previous 5 years. Rapid declines in total biome NPP from 2019 to 2020–2021 were estimated for all biomes except those in the tropical forest zones. Trends in NPP in areas of the largest wildfires in North America that burned between 2012 and 2021 were further examined to assess recovery of vegetation and the resiliency of ecosystems during the extreme 2020–2021 drought period. Results implied that warmer, drier climate conditions are leading to lower tree regeneration after wildfires in the past decade, compared to the decades of the 1980s and 1990s.

## 1. Introduction

Net photosynthetic accumulation of carbon by plants, also known as net primary production (NPP), is driven by vegetation capture of solar radiation, and this carbon supports most biotic processes on Earth (Potter et al., 1993). Climatic regulation of terrestrial NPP fluxes is an issue of central relevance to human societies and economies, particularly to the extent that NPP can be managed to provide adequate food and fiber to meet the needs of human populations (Jay et al., 2016).

Across North America, many extreme weather events and wildfires over the past decade have caused major disturbance incidents and hundreds of billions of dollars in damage to infrastructure (Hsiang et al., 2017). There has been a steep rise since 2012 in severe drought periods, longer wildfire seasons in the western region, coastal flooding and extremely heavy precipitation events in the southern and eastern regions of North America (NOAA NCEI, 2023). For instance, extreme drought conditions were persistent throughout 2020 and 2021 across the western regions of the United States and Canada. An historic heat wave also developed for many days in 2021

**Supervision:** Christopher Potter
**Validation:** Christopher Potter, Stephanie Pass
**Visualization:** Christopher Potter
**Writing – original draft:** Christopher Potter, Stephanie Pass
**Writing – review & editing:** Christopher Potter, Stephanie Pass, Rachel Ulrich

across the Pacific Northwest, extending well into Canada, setting numerous all-time high temperature records across the region (Smith, 2022). Category 4 Hurricanes Ida (August 2021) and Ian (August 2022) lashed the Gulf Coast states with destructive wind speeds and widespread flooding.

Preceding these extreme weather periods, the 2015/16 El Niño broke warming records in the central Pacific, represented by the NINO3.4 and NINO4 indices (Stockdale et al., 2017). At its peak in November 2015, the NINO3.4 sea surface temperature (SST) anomaly reached 3.0°C, breaking the previous record of 2.8°C set in January 1983. This El Niño event generally led to warmer-than-average conditions across central North America. However, major winter storm systems still occurred, including a flash flooding in Texas at the end of December 2015 and numerous tornadoes in the southern United States at the end of February, 2016. An historic blizzard struck the northeastern United States in late January, 2016. Nevertheless, the impact of such extreme climate shifts on continental-scale NPP has not been closely studied for the period of the past several years.

To address this knowledge gap, the CASA (Carnegie-Ames-Stanford Approach) carbon cycle model (Potter et al., 1993, 2012) predicts the monthly NPP flux of atmospheric carbon dioxide (CO2) between plants and soils on a global scale using satellite image inputs from the NASA Moderate Resolution Imaging Spectroradiometer (MODIS). CASA is the only global carbon model that has consistently used MODIS and Landsat products for land cover classes and green vegetation indices as monthly inputs to drive the prediction of NPP and soil $CO_2$ emissions in the terrestrial biosphere. It is the most well-integrated model of the global carbon and water cycles with high-level products from NASA satellite remote sensing missions. Moreover, the nominal 8-km grid cell resolution of the CASA model enables localized studies of ecosystem carbon and water fluxes of interest to public sector stakeholders working at nearly every organizational level.

Recently, the CASA model has been a cornerstone of science investigations to evaluate results of $CO_2$ fluxes from NASA's Orbiting Carbon Observatory (OCO-2 and OCO-3) mission, as illustrated in the publication by Philip et al. (2019). These OCO-2 inverse model results for validating observed $CO_2$ patterns in the atmosphere used CASA outputs as prior conditions for the land surface $CO_2$ flux contribution. The CASA model is also the foundation for the CASA-GFED (Global Fire Emissions Database) model, which estimates monthly NPP and soil heterotrophic respiration globally, along with biomass burning emissions of $CO_2$ each year (Randerson et al., 2018).

CASA NPP model calibration has been validated repeatedly, first globally by comparing predicted annual NPP to more than 1900 field measurements of NPP (Potter et al., 1993, 2012). Interannual NPP fluxes from the CASA model have been reported (Behrenfeld et al., 2001) and validated against multiyear estimates of NPP from field stations and tree rings (Malmström et al., 1997). The CASA model has been validated against field-based measurements of ecosystem $CO_2$ fluxes and carbon pool sizes at multiple boreal forest sites in North America (Amthor et al., 2001; Hicke et al., 2002; Potter et al., 2001) and against atmospheric inverse model estimates at the global scale (Potter et al., 2003). More recently, Jay et al. (2016) validated CASA NPP estimates using 17 Ameriflux tower flux sites located across North America.

In the present study, the CASA model has been applied to the North American continent over the period of 2015–2022. The primary research questions posed in this study were:

- How have variations in precipitation and air temperature resulted in drought impacts on NPP in all the ecoregions of North America over the study period?
- How have large wildfires over the past decade affected NPP in selected ecoregions of North America?

We focused on the main growing season months of May to August in North America to more precisely isolate and evaluate the impacts of variable precipitation totals and extreme heat events on plant production. CASA model outputs were summed and averaged for growing season NPP flux of $CO_2$ (Potter et al., 1993) in 13 ecoregion biomes of North America from 2015 to 2022.

## 2. Methods

### 2.1. CASA NPP Algorithms

Monthly net vegetation carbon fixation patterns, or NPP, were computed from the CASA model by using the concept of light-use efficiency (Monteith, 1972). NPP is calculated as a product of time-varying solar radiance ($S_r$), precipitation, air temperature, the Enhanced Vegetation Index (EVI) from MODIS satellite imagery, and a

constant light utilization efficiency term ($e_{max}$) that is modified by time-varying stress temperature (T) and moisture (W) (Potter et al., 1999).

$$NPP = S_r \, EVI \, e_{max} \, T \, W$$

Based on calibration using field estimates of NPP from across the globe, the constant $e_{max}$ term was set at 0.55 C $MJ^{-1}$ $S_r$ (Potter et al., 1993, 2012).

The air temperature (T) stress scalar for CASA NPP computation is computed with reference to derivation of optimal temperatures (Topt) for plant production. The Topt setting will vary by latitude and longitude, ranging from near 0°C in the Arctic to the middle thirties in low-latitude deserts. For this study, Topt has been updated using air temperatures for the past several years (2015–2022). The soil moisture availability stress scalar (W) is estimated from monthly water deficits, based on a comparison of moisture supply (precipitation and stored soil water) to potential evapotranspiration (PET) demand using the method of Priestley and Taylor (1972).

Evapotranspiration is connected to water content in the soil profile layers, as estimated using the algorithms described by Potter et al. (1999). The soil model design includes three-layer (M1–M3) heat and moisture content computations: surface organic matter (SOM), topsoil (0.3 m), and subsoil to rooting depth (1–2 m). These layers can differ in soil texture, moisture holding capacity, and carbon–nitrogen dynamics. Water balance in the soil is modeled as the difference between precipitation or volumetric percolation inputs, monthly estimates of PET, and the drainage output for each layer. Inputs from rainfall can recharge the soil layers to field capacity. Excess water percolates through to lower layers and may eventually leave the system as seepage and runoff. Freeze–thaw dynamics with soil depth operate according to the empirical degree-day accumulation method (Jumikis, 1966), as described by Bonan (1989).

### 2.2. Global Input Data Sets

#### 2.2.1. NCEP

Global monthly data from the NCEP-DOE Reanalysis 2 data set was acquired for the years 2015–2022 via the National Oceanic and Atmospheric Administration (NOAA) data portal (Kanamitsu et al., 2002). Monthly mean air temperatures, air maximum temperatures, air minimum temperatures, mean solar radiation flux, and mean precipitation rate files were acquired for model inputs.

In order to prepare the NCEP data for the CASA model, unit conversions were necessitated. First, all of the NCEP files were reprojected into the Mollweide (ESRI:54009) spatial reference system with 8-km size cells and passed through a 20 × 20 focal smoothing filter. NCEP temperature values were converted from degrees kelvin to degrees Celsius. Solar radiation flux was converted from watts per square meter (W $m^2$) to Megajoules (MJ $mo^{-1}$), taking into account average daylight minutes per month for North America. Precipitation values were converted from kg $m^{-2}$ to cm $month^{-1}$.

#### 2.2.2. MODIS EVI

Terra MODIS data sets for the years 2015–2022 were obtained from NASA's Land Processes Distributed Active Archive Center site (LP-DACC) (Didan, 2015). One 16-day Enhanced Vegetation Index (EVI) file was chosen for each month from the MOD13C1 Version 6 data repository to obtain CASA input data. The global composite (cloud-adjusted) MODIS imagery was converted to 8-km resolution and into a Mollweide spatial reference system.

#### 2.2.3. MODIS Land Cover

The MODIS 1-km land cover map (Friedl et al., 2002) was aggregated to 8-km pixel resolution and used to specify the predominant land cover class. These classes were used to assign the soil rooting depth settings in CASA as either forest, shrubland, or grassland (Potter et al., 2012).

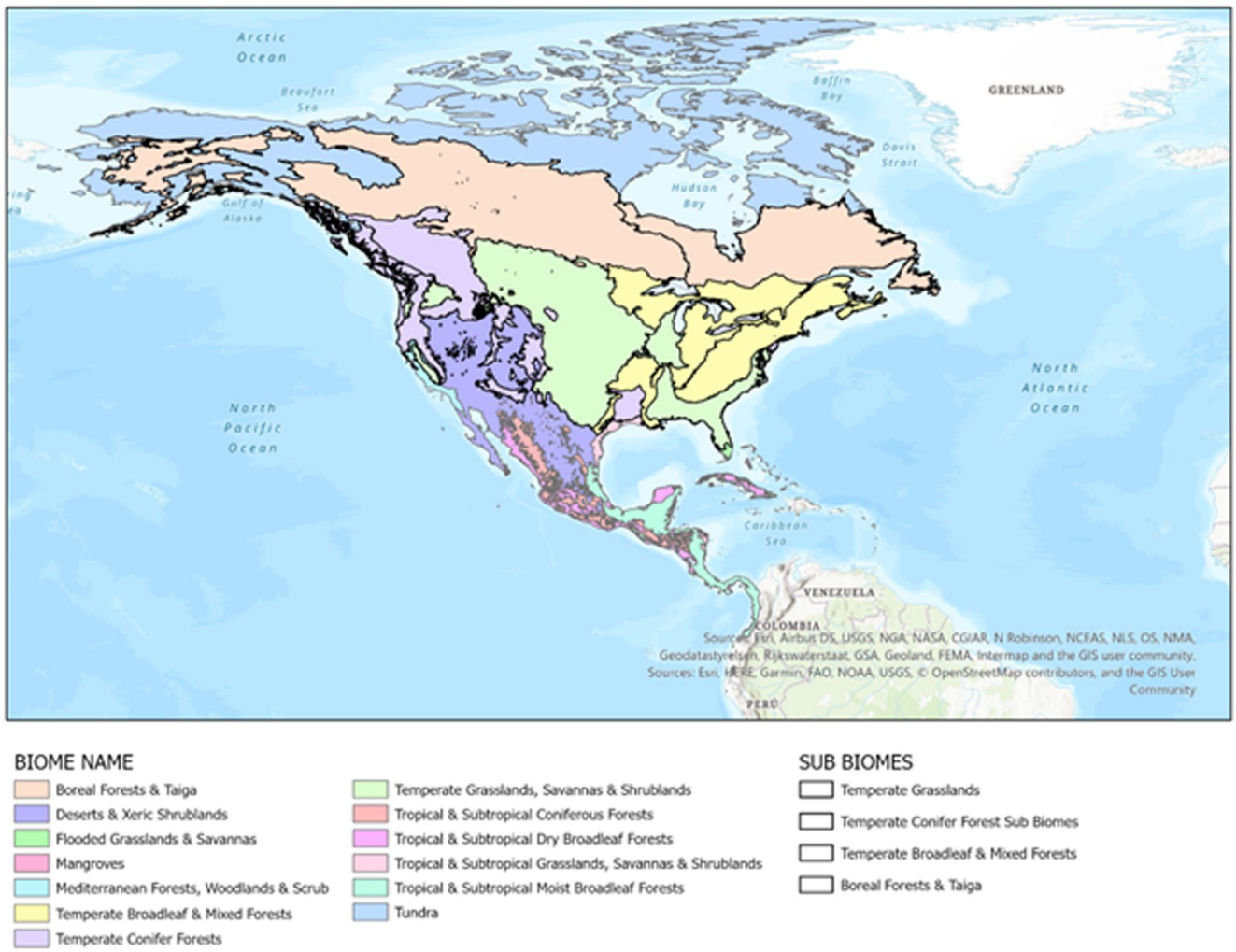


**Figure 1.** Map of the 13 ecoregion biomes (Olson et al., 2001) used to analyze growing season sum NPP values in North America for the years 2015–2022. Four biomes were further broken down into sub-biomes for additional analysis.

### 2.3. Statistical Methods

Monthly NPP files for the years 2015–2022 were output from the CASA model. We selected the growing season (May through August) NPP files to further analyze with R (R Core Team, 2022). The monthly NPP growing season values were summed into yearly values using the raster package in R (Hijmans, 2023). Polygon shapefiles of the selected ecoregion biomes and sub-biomes (Olson et al., 2001; Figure 1, Tables 1 and 2) were used to mask the NPP rasters for further analysis. NPP growing season averages and sums were ascertained from the files using the raster package's cellStats function (Hijmans, 2023). The 8-km cell size was taken into account to obtain the total summed grams of carbon per biome. A similar process was also carried out to obtain average yearly rainfall and yearly mean air temperature values from our prepared NCEP files. Summed growing season NPP values were also computed for the largest (in area) wildfires that occurred in North America during the years 2012–2021, using fire perimeter data sets from Eidenshink et al. (2007).

We used the quantile function from the stats package (version 4.2.2) in R (R Core Team, 2022) to calculate the quantiles around the mean for average growing season NPP, average yearly precipitation (cm $y^{-1}$), and average air temperature (C) for each biome. We used the 25th and 75th percentiles to identify the interquartile range (IQR) to plot and demonstrate the spread of the values for each biome. These quantiles are represented as error bars for the plotted mean data for the NPP ecoregion biomes, yearly mean precipitation, and yearly mean temperature. The R packages ggplot2 (Wickham, 2016) and ggmatplot (Liang et al., 2021) were used to visualize the data.

**Table 1**
*Thirteen Ecoregion Biomes and Their Corresponding Area Coverage in North America*

| Biomes | km$^2$ |
|---|---|
| Boreal Forests and Taiga | 5,375,552 |
| Deserts and Xeric Shrublands | 2213.248 |
| Flooded Grasslands and Savannas | 24,384 |
| Mangroves | 77,312 |
| Mediterranean Forests, Woodlands, and Scrub | 129,344 |
| Temperate Broadleaf and Mixed Forests | 2,604,928 |
| Temperate Conifer Forests | 1,988,928 |
| Temperate Grasslands, Savannas, and Shrublands | 3,606,080 |
| Tropical and Subtropical Coniferous Forests | 576,384 |
| Tropical and Subtropical Dry Broadleaf Forests | 513,792 |
| Tropical and Subtropical Grasslands, Savannas, and Shrublands | 113,600 |
| Tropical and Subtropical Moist Broadleaf Forests | 660,096 |
| Tundra | 3,911,616 |

To better understand growing season NPP response to drought we further analyzed the difference by looking at the relative change (in percent) of NPP from 2019 to 2020 and from 2019 to 2021 using the R's raster package (Hijmans, 2023). We used drought zone polygons from the Drought Monitor project (Svoboda et al., 2002) to understand the percent change of NPP values in the specified drought regions. To analyze for significant differences in zonal samples of the NPP percent change values, non-parametric statistical tests were performed. Due to the tendency of NPP values to be non-normally distributed, sample tests were performed in R using the stats package's Kruskal-Wallis test function and pairwise Wilcoxon.test function (R Core Team, 2022). The Kruskal-Wallis Rank Sum Test was used to determine whether or not there was a statistically significant difference between the medians of three or more sample groups. The pairwise Wilcoxon rank sum test was used to compare all of the independent samples to one another to evaluate differences in the sample distributions. The median value for each sample was ascertained by using R's summary function from the statistics package (R Core Team, 2022).

**Table 2**
*Nineteen Sub-Biomes and Their Corresponding Area Coverage in North America*

| Sub-biomes | km$^2$ |
|---|---|
| Alaskan Boreal Forests | 519,424 |
| Western Canada Boreal Forests | 2,992,256 |
| Eastern Canada Boreal Forests | 1,863,872 |
| Western Grasslands and Savannas | 146,112 |
| Central Shortgrass Prairies | 2,629,312 |
| Eastern Grasslands and Savannas | 830,656 |
| Northern Temperate Broadleaf Forests | 1,228,288 |
| Eastern Temperate Broadleaf Forests | 1,028,480 |
| Southern Temperate Broadleaf Forests | 348,160 |
| Pacific Coast Conifer Forest | 260,992 |
| Northern California Conifer Forest | 273,024 |
| Rocky Mountains Conifer Forest | 1,288,448 |
| Eastern Conifer Forest | 166,464 |
| Beringia Lowland Tundra | 152,704 |
| Brooks-British Range Tundra | 160,512 |
| Canadian Low Arctic tundra | 837,696 |
| Canadian Middle Arctic Tundra | 982,208 |
| Interior Yukon-Alaska Alpine Tundra | 152,448 |
| Ogilvie-MacKenzie Alpine Tundra | 302,336 |

## 3. Results

### 3.1. CASA NPP by Biome

Average growing season NPP (g C m$^{-2}$; Figure 2) was shown to be consistently highest in the Tropical and Subtropical Moist Forest biome with a range of 277–313 g C m$^{-2}$, followed by the Temperate Broadleaf Forest with a range of 241–249 g C m$^{-2}$, and the Tropical and Subtropical Dry Forest biome with 219–238 g C m$^{-2}$. Desert and Tundra biomes showed the lowest growing season average NPP, with respective ranges of 65–75 g C m$^{-2}$ and 57–70 g C m$^{-2}$. All other biomes showed average growing season NPP at intermediate levels of plant production.

Owing to their extensive area cover in North America, the Temperate Broadleaf Forest and Boreal Forest biomes had the highest total growing season NPP flux, each at between 600 and 730 Tg C, compared to the next highest biome, the Temperate Grasslands and Savanna (including most croplands and rangelands), with total growing season NPP between 560 and 680 Tg C. Tundra and Temperate Conifer Forest biomes each showed total growing season NPP between 220 and 300 Tg C, and tropical and subtropical

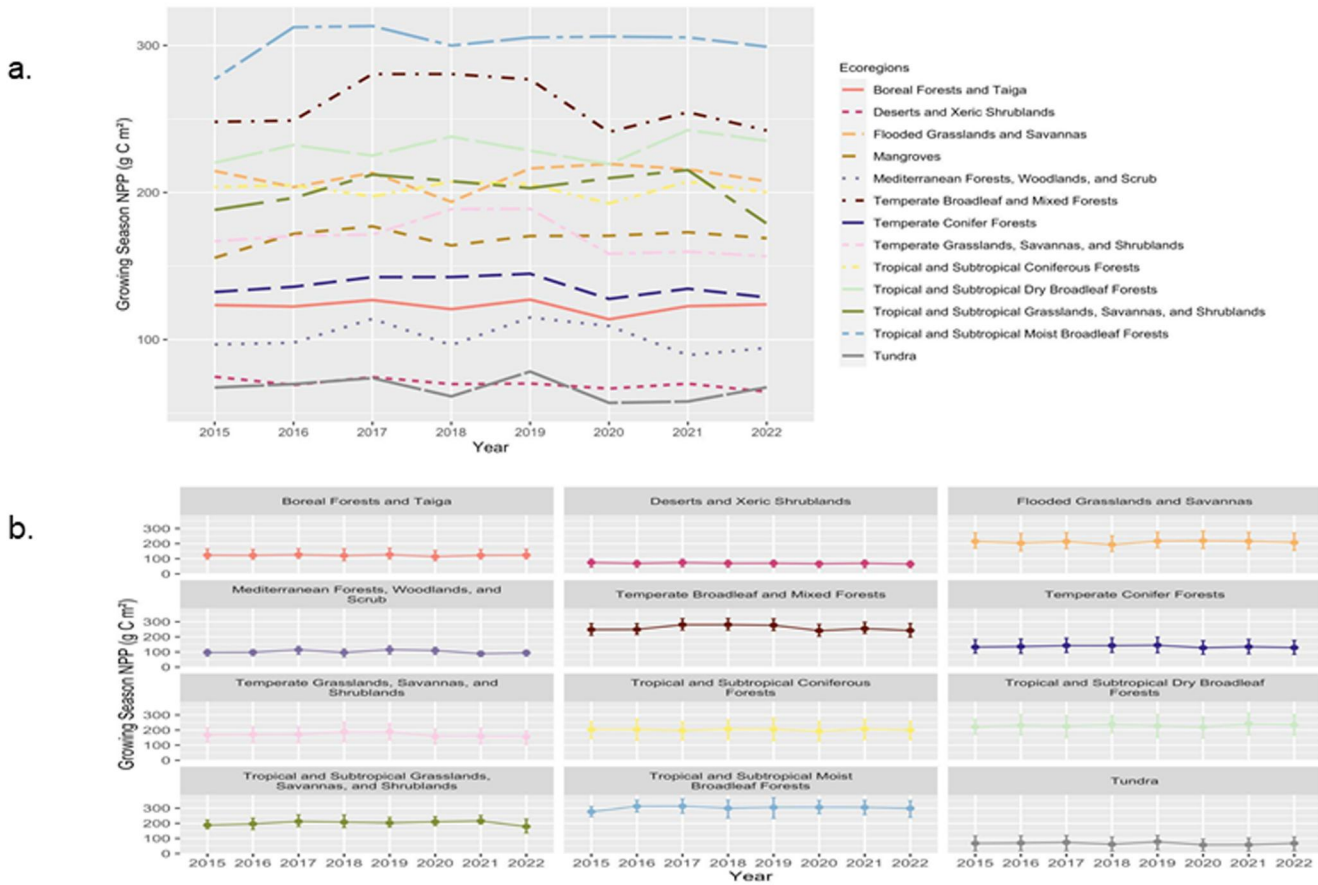


**Figure 2.** (a) Comparison of the average growing season NPP (g C $m^{-2}$) for 13 North American biomes for the years 2015–2022. (b) Average growing season NPP (g C $m^{-2}$) for 12 North American biomes from 2015 to 2022 displayed with their Interquartile Range.

grasslands showed total growing season NPP between 210 and 250 Tg C. All other biomes were estimated to individually have a total growing season NPP lower than 150 Tg C.

Over the study period of 2015–2022, several notable high and low periods were identified for growing season NPP totals in certain biomes (Figure 3). Both total Temperate Broadleaf and Boreal Forest production shifted from relatively high average values (640–730 Tg C) in 2015 through 2019 to low levels of less than 630 Tg C in 2020, typically representing a loss of 10%–14% of growing season NPP flux across these large biome areas from 2019 to 2020. This rapid decline in growing season NPP from 2019 to 2020–2021 was also estimated for the Temperate Grasslands and Savanna, Temperate Conifer Forest, and Tundra biomes. The Boreal Forest and Tundra biome areas recovered their growing season NPP totals to the greatest degree in 2022. The total growing season NPP in all tropical and subtropical biomes varied relatively little from year to year.

For a more detailed examination of CASA model NPP predictions within North American biomes, sub-biome comparisons for total NPP fluxes per year are presented in Figures S1–S7 in Supporting Information S1 section of this paper.

### 3.2. Precipitation and Temperature Variations by Biome

Annual precipitation totals in the Boreal Forest biomes declined from a high average value of 95 cm $y^{-1}$ in 2015 and 2016 to a low average precipitation total of 87 cm $y^{-1}$ in 2021, followed by an increase to 90 cm $y^{-1}$ in 2022 (Figure 4). Annual precipitation totals in the Tundra, Temperate Broadleaf Forest, Temperate Grasslands, and Mediterranean Forest and Woodland biomes all declined from high average values in 2018 or 2019 to markedly drier years from 2020 to 2022. The Flooded Grasslands and Savannas biome decreased from 200 cm $y^{-1}$ in 2020

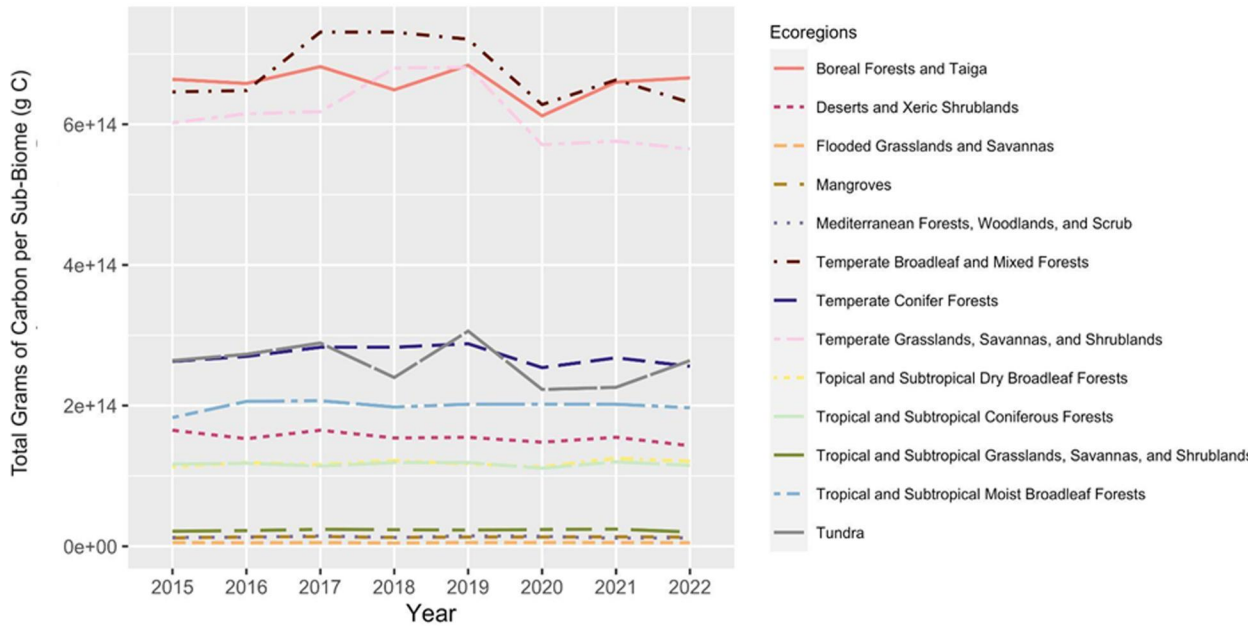


**Figure 3.** Comparison of total growing season NPP (g C) per biome from 2015 to 2022.

to a low of 124 cm $y^{-1}$ in 2021, and then experienced a marked increase to 241 cm $y^{-1}$ in 2022. Annual precipitation totals in the Temperate Conifer Forest biome varied from high average values of 108 cm $y^{-1}$ in 2021 to markedly drier years from 2019 to 2020 of around 92 cm $y^{-1}$. Annual precipitation totals in most of the tropical and subtropical biomes were consistently highest in 2022 and lowest in 2019 and 2020.

Annual average air temperatures increased slightly over the study period of 2015–2022 in the Tundra biome (Figure 5). Average annual temperatures remained relatively constant in all the tropical and subtropical biomes. The years 2018 and 2019 were the relatively coolest years on average in most temperate biomes. However, 2019 was the warmest year for the Tundra biome, and a notable warming trend was observed between 2020 and 2022.

### 3.3. CASA NPP Response to Drought

Nine of the 13 North American biomes experienced a decline in growing season NPP (g C) from 2019 to 2020 (Figure 6a). The Tundra biome experienced the largest relative change (in percent) in NPP from 2019 to 2020 with a 27% overall decline. The Temperate Grasslands and Savannas biome experienced the next largest decrease in NPP from 2019 to 2020 with an overall decrease of 16% followed by the Temperate Broadleaf and Mixed Forests biome which experienced an overall 13% decline.

Six of the13 biomes experienced a decline in growing season NPP (g C) from 2019 to 2021 (Figure 6b). Again the Tundra biome had the largest overall decline in NPP with a relative decrease of 26% followed by the Mediterranean Forest Biome with a decrease of 22% and the Temperate Grasslands, Savannas, and Shrublands biome which declined 15% overall.

To aid in understanding what caused these changes in NPP between 2019 and 2021, the North American Drought Monitor (NADM; Svoboda et al., 2002) maps the state of drought conditions (example in Figure 7, Table 3) for most of the continental land mass on a monthly basis. NADM severity categories (0–4) are based on six key physical indicators and many supplementary indicators. The key indicators are the Palmer Drought Severity Index, Soil Moisture Model Percentiles, U.S. Geological Survey (USGS) Daily Streamflow Percentiles, Percent of Normal Precipitation, Standardized Precipitation Index, and a remotely sensed Satellite Vegetation Health Index. The majority of these indicator data sources for mapping NADM drought severity classes are not used in

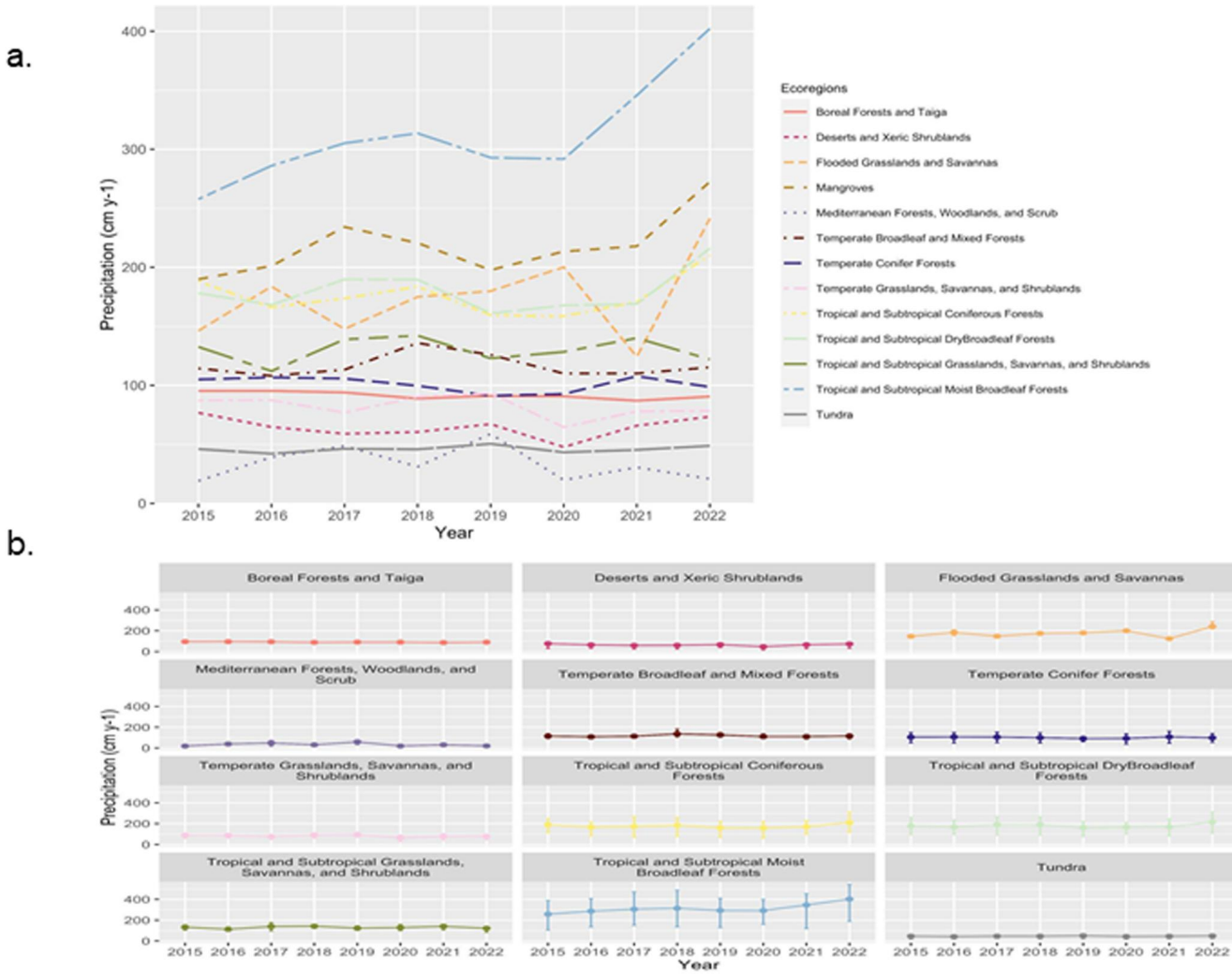


**Figure 4.** (a) Annual precipitation totals in cm $y^{-1}$ for 13 North American biomes for the years 2015–2022. (b) Annual precipitation totals in cm y-1 for North American biomes from 2015 to 2022 displayed with their Interquartile Range.

the CASA model as inputs, which makes the comparison of products from these two model results essentially independent.

The categories of drought severity used in the NADM are each associated with the percentile chance of occurring in any given year out of 100 years, as specified below by Svoboda et al. (2002).

The Kruskal Wallis test was used to compare independent samples (in this case, the five NADM drought category zones shown in Figure 7) for NPP change between 2019 and 2021, to determine whether or not there was a statistically significant difference between the medians of the five sample groups. The null hypothesis was that there is no significant difference between NPP samples among the five drought severity zones and the alternative hypothesis was that some or all of the severity groups are different. Kruskal Wallis test results with $p < 0.001$ showed that the null hypothesis could be rejected and that there was a significant difference in NPP change (2019–2021) samples among the drought severity zones. The Wilcoxon ranks test compared each of the five drought category zone samples for NPP change against all the other zones samples. Results showed that NPP change samples in all of the drought severity zone categories were statistically different (all comparisons at $p < 0.001$) from one another, and hence we again rejected the null hypothesis that the sample medians were the same.

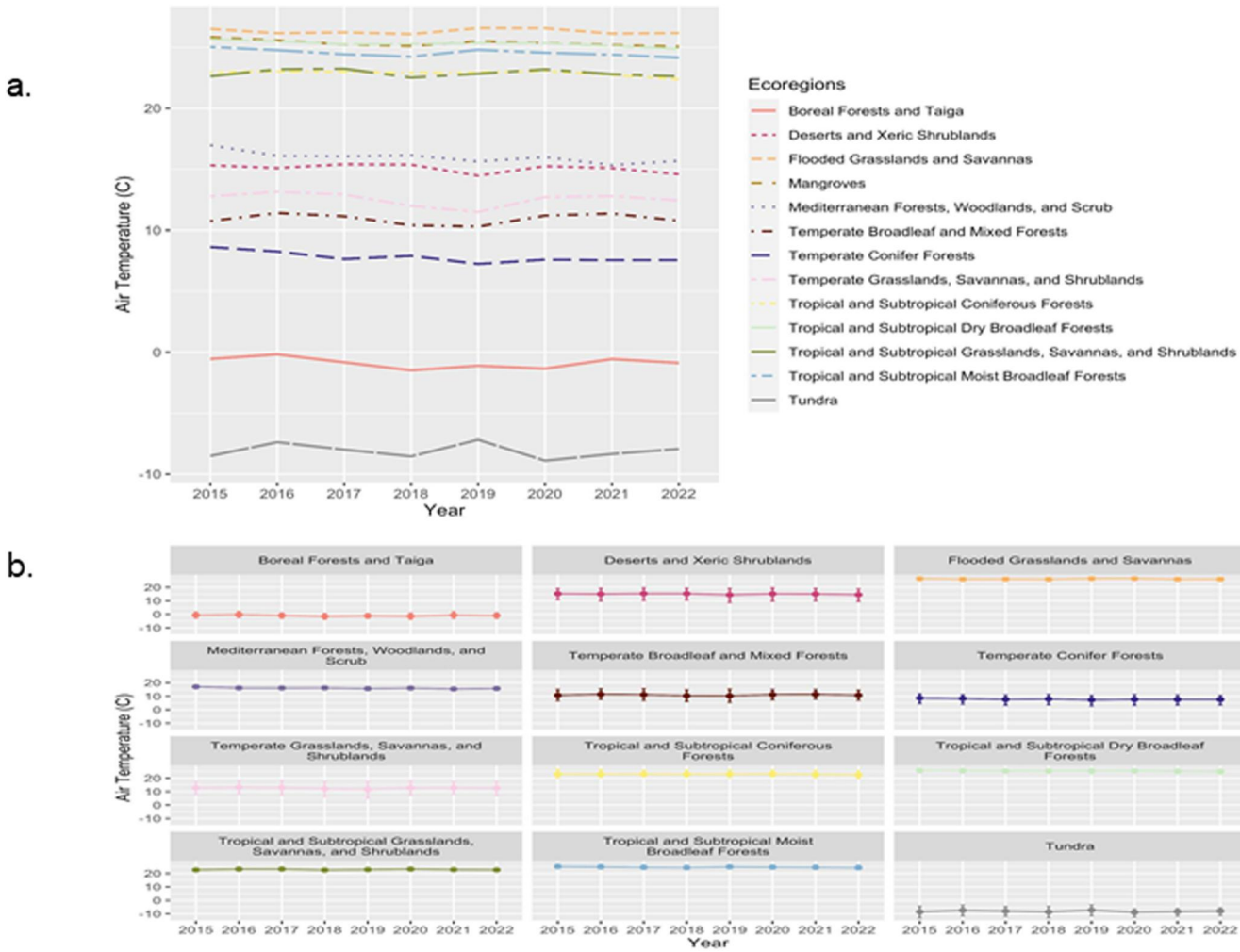


**Figure 5.** (a) Annual average air temperatures (degrees Celsius) for the 13 North American biomes for the years 2015–2022. (b) Annual average air temperatures (degrees Celsius) for North American biomes from 2015 to 2022 displayed with their Interquartile Range.

The median values for the percent change in growing season NPP from 2019 to 2021 was shown to be highest for the D3 and D4 drought zones at −18% to −24% (Table 4). The median for the percent change in growing season NPP was nearly as high for the D2 drought zone at −17.8%. The regions of exceptional drought severity (D4) in 2021 most impacted by loss of NPP in the preceding two years were as follows: the Snake River Valley of eastern Washington and Oregon, the southern Cascade Mountain range, all of central California, the northern Rocky Mountains, northeastern Montana, and southeastern Manitoba. Each of these D4 regions were connected by a 50–200 km buffer zone of extreme drought severity (D3) in 2021.

### 3.4. CASA NPP for Large Wildfires

The largest wildfires (in areas burned) in the lower 48 states of the United States that had occurred between the years 2012 and 2014 (Figures 8 and 9) commonly showed increasing growing season NPP totals between the years 2015–2019, after which time, most total growing season plant production in the burned areas declined notably in 2020–2021 and recovered only partially in 2022. This pattern of a disruption of NPP recovery starting in 2020 from recent large wildfire incidents was particularly noteworthy for the Ash Creek (northern shortgrass prairie sub-biome), Holloway (shrubland-steppe sub-biome), Rush (shrubland-steppe sub-biome), and Whitewater-Baldy (temperate conifer forest) fires of 2012.

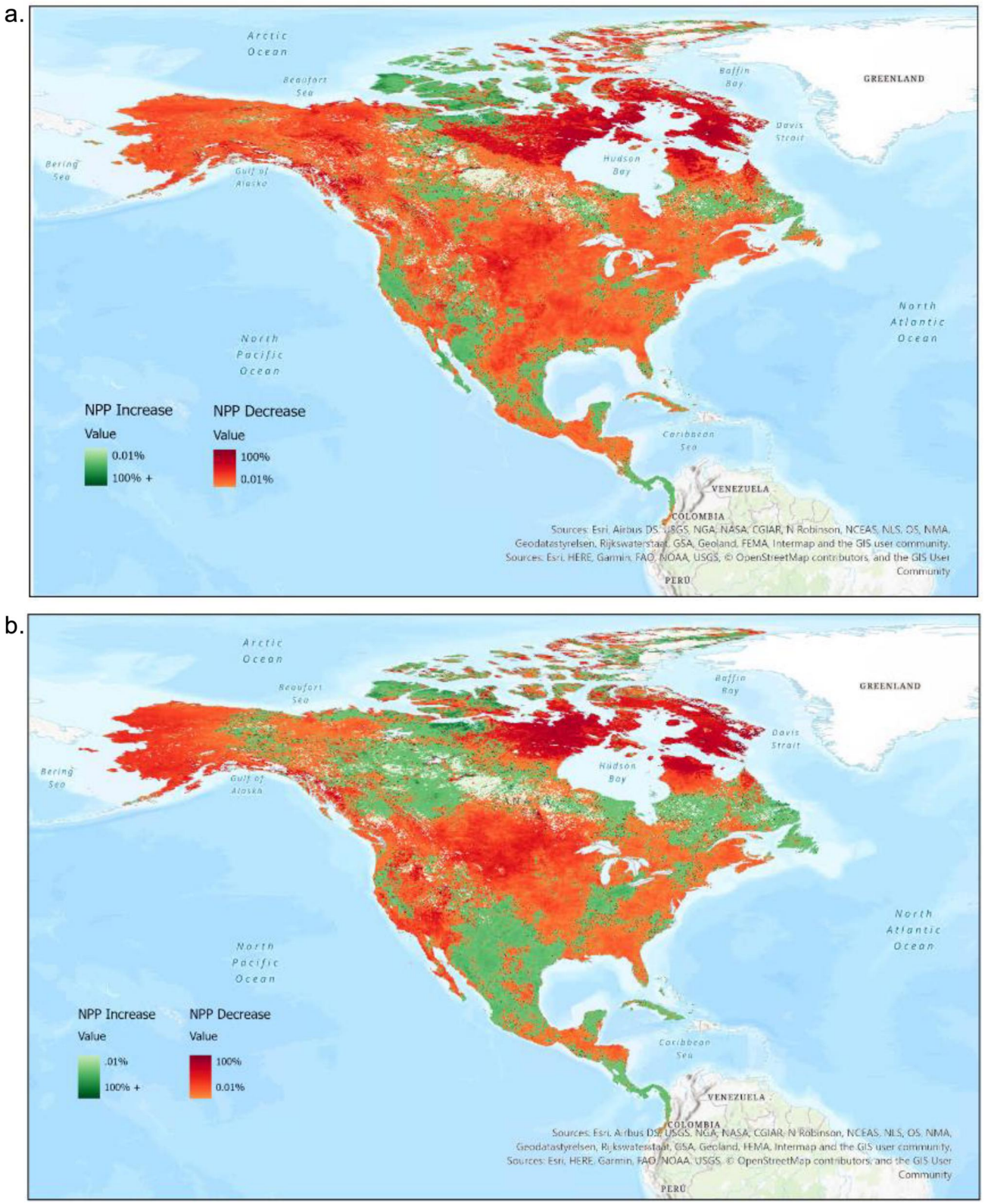


**Figure 6.** (a) Map of North America depicting the relative change (in percent) of NPP from 2019 to 2020. (b) Map of North America dep icting the relative change (in percent) of NPP from 2019 to 2021.

The large wildfires in North America that had occurred between the years 2016 and 2022 (Figure 10) commonly showed sharp declines in growing season NPP totals in the year following the wildfire incident, after which, total growing season plant production in these recently burned areas recovered partially in 2022. Notably, the largest recent fire in the region and in the state's (California's) history, the 2020 August Complex with a burned area of 1,032,648 acres (4,180 $km^2$), showed a 57% loss of total NPP from 2020 to 2021 in burned areas dominated by woodlands of the Coast Range ecoregion in northwestern California. In comparison, NPP decreased by 60% following the 2020 North Complex fire, which burned in the Plumas National Forest of northern Sierra-Nevada ecoregion. The Creek Fire in the southern Sierra-Nevada range also experienced a notable decrease in NPP with a 42% decline from 2020 to 2021.

## 4. Discussion

The results from this CASA ecosystem modeling study imply that there have been major variations in and perturbations to NPP fluxes in North America over the period of 2015–2022, due primarily to extreme and widespread droughts and owing to some of the largest and most severe wildfires ever recorded on the continent. Modest, gradual increases in average NPP across most biomes from 2015 to 2019 were followed by typical declines of 15%–25% of growing season NPP from 2019 to 2021. The Tundra biome experienced the largest relative change in NPP from 2019 to 2021, followed by the Temperate Grasslands and Savannas biome and the Temperate Broadleaf and Mixed Forests biome.

Consistent with our newest CASA model results, a number of recent regional studies have reported that "greening" of the arctic tundra and a shift toward shrub dominance has occurred, coincident with rapid increases in summer air temperatures over the past several decades. In a study of arctic greening patterns, Bonney et al. (2018) examined the Landsat Normalized Difference Vegetation Index (NDVI) time-series from 1984 to 2016 for an area spanning the transition from sub-Arctic boreal forest to Low Arctic tundra in central Canada. Results indicated that 25% of the study area experienced increasing NDVI, particularly at higher latitudes. Dense shrublands and open woodlands showed the highest levels of greening.

Berner et al. (2020) conducted a study using satellite imagery measuring "greening" in a section of forest to tundra biomes in Central Canada. They found that the largest increases were occurring in the northern tundra zone with shrub and lichen vegetation. These results are consistent with the CASA model that shows an overall trend in greening in a similar study area of the Canadian Low Arctic Tundra sub-biome, with an overall 17% NPP increase from 2015 to 2022. The sub-biome's most productive NPP year and warmest temperatures were experienced in 2017 followed by a second most productive NPP year and second warmest average air temperatures in 2022. Overall the tundra biome had its warmest temperatures, highest amount of precipitation, and most productive NPP in the growing season of 2019.

Over the study period of 2015–2022, the largest biome in area coverage, the Boreal Forest and Taiga biome, transitioned from relatively high total NPP values in 2015 through 2019 to lower total NPP afterward, representing a loss of 11% of growing season NPP flux from 2019 to 2020 in the western Canadian sub-biome and a loss of 18% in the Alaskan sub-biome. Along similar lines, it was reported by Mariën et al. (2021) that, in recent decades, the rate of biomass change decreased significantly in western Canada (Alberta, Saskatchewan, and Manitoba), but there were no significant changes in biomass accumulation rates for boreal forests of eastern Canada (Ontario and Quebec). These authors surmised that drought-induced water stress is the dominant cause of an observed reduction in the boreal forest biomass carbon sink, suggesting that western Canada's forests may become net carbon sources if the climate change related droughts continue to intensify.

For temperate deciduous forests, Mariën et al. (2021) investigated the impact of drought on tree mortality. These authors found that low precipitation and high temperatures were associated with a higher rate of mortality for tree saplings and foliage in mature trees. The CASA results from this study indicated that the Temperate Broadleaf and Mixed Forest biome experienced its two highest years of precipitation in 2018 and 2019 followed by a 13% decline in annual precipitation in 2020. Growing season NPP values increased 20% from 2017 to 2018 and then decreased 13% from 2019 to 2020, following these annual precipitation variations. Temperatures were also the coolest in 2018 and 2019 over the 7-year study period.

A study by Berner et al. (2017) measured the impact of precipitation on forests in the western United States. They found that these forest ecoregions were susceptible to changes in precipitation and declined in

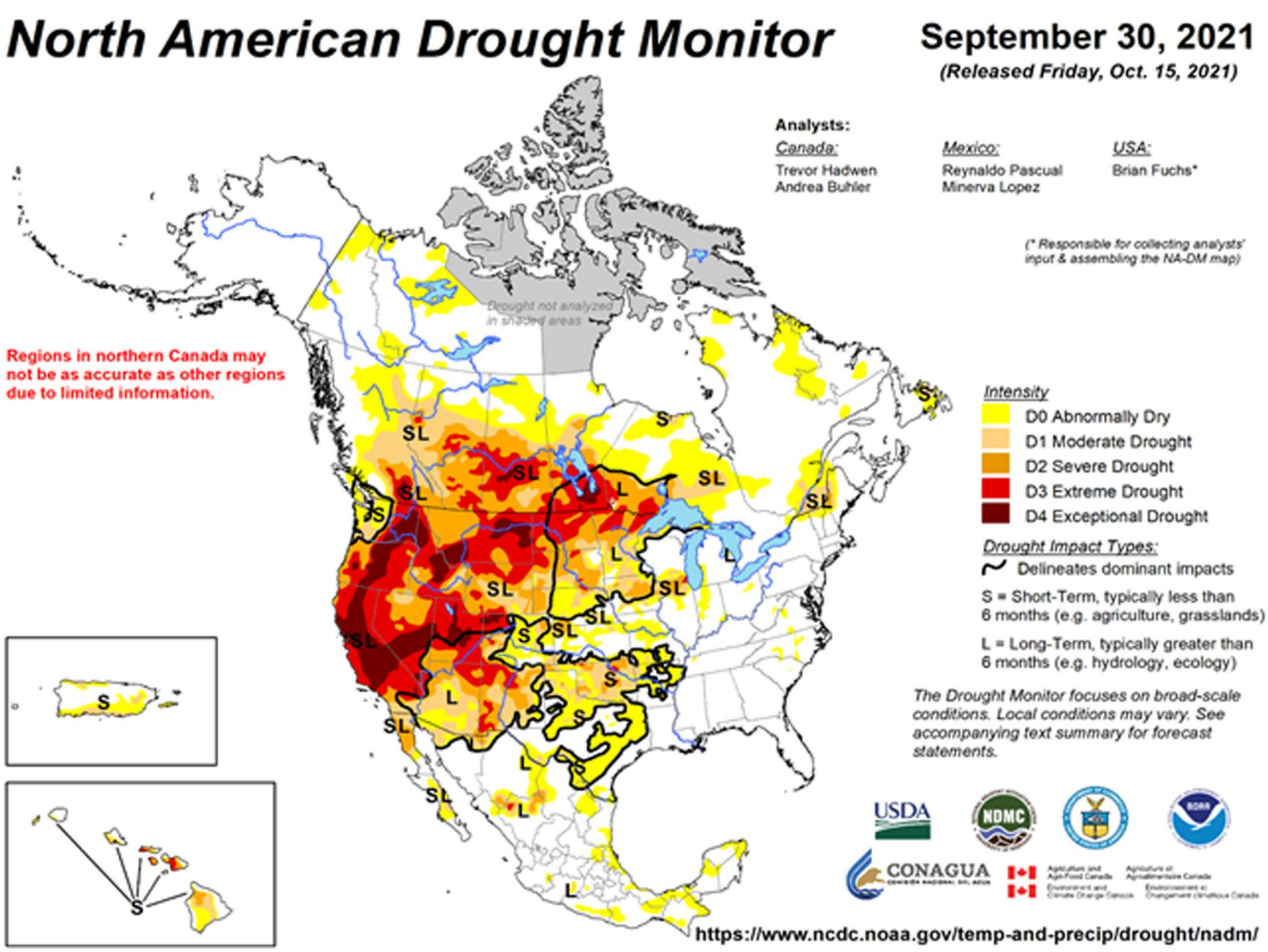


**Figure 7.** Map of drought severity categories across North America in September 2021. Reprinted from "North American Drought Monitor Maps."

productivity with lower water availability. The authors reported that current climate models predict lower precipitation rates and higher temperatures that will most likely result in reduced NPP in these regions, especially in drier areas. In the CASA model results, the Temperate Conifer Biome overall experienced gradual increases in NPP from 2015 to 2019 and then in 2019 the biome had its coolest air temperatures and lowest year of average rainfall in 2019. After this low precipitation period, the biome proceeded to have its lowest year of NPP in 2020. The largest Temperate Conifer sub-biome, the Rocky Mountain region, experienced its lowest year of NPP in 2020 following its two driest years of precipitation over the study period in 2019 and 2020.

**Table 3**
*Categories of Drought Severity Used in the NADM*

| Category | Drought condition | Percentile chance |
|---|---|---|
| D0 | Abnormally Dry | 20 to <30 |
| D1 | Drought-moderate | 10 to <20 |
| D2 | Drought-severe | 5 to <10 |
| D3 | Drought-extreme | 2 to <5 |
| D4 | Drought-exceptional | <2 |

Several previous reports of drought impacts on cropland production trends support our NPP change results in the temperate grasslands biome. According to the National Drought Mitigation Center (NDMC), the percentage of alfalfa acreage affected by drought during the summer of 2021 was the largest in the past decade. As drought in the United States continued into 2022, approximately 12% of alfalfa hay acreage was experiencing severe or exceptional drought conditions. The Public Policy Institute of California reported in 2022 that irrigation water shortages in California's Central Valley led to 395,000 acres of cropland idled because of the 2021 drought, with the majority of these unplanted fields in the Sacramento Valley. According to the U. S. Department of Agriculture (USDA) National Agricultural Statistics Service (NASS), crop conditions in the state of Washington were rated poor to very poor in 2021 for

**Table 4**
*The Median NPP Percent Change Values From 2019 to 2021 in the Five Drought Intensity Zones*

| Drought intensity | Median value |
|---|---|
| D0 | −1.6 |
| D1 | −5.7 |
| D2 | −17.8 |
| D3 | −24.9 |
| D4 | −18.6 |

rangeland and pastures (97%), spring wheat (88%), and barley (61%), while 60%–80% of rangeland and pastures in both Oregon and Idaho were rated poor to very poor.

According to Statistics Canada (2021), their croplands produced less wheat, canola, barley, soybeans and oats in 2021 compared with 2020. It was reported that lower crop yields were driven largely by drought conditions in western Canada. Extremely hot and dry weather impacted crop development during the growing season in central Canada, whereas in eastern Canada, temperatures were near normal throughout much of the growing season.

A report by Umphlett et al. (2022) for the Northern Plains of the United States and the Canadian Prairies documented that, prior to the onset of the 2020–2021 drought, portions of these grassland regions were emerging from one of the most extreme wet periods on record. In 2020, drought conditions initially developed in the spring, and slowly intensified and expanded to encompass much of the region by the end of 2020. Extremely dry conditions persisted over the winter and spring of 2020–2021, with intense heat building during the summer months. Around 55 million acres of cropland and 50 million acres of rangeland were adversely impacted, and livestock herds were reduced by 15% across the Canadian Prairies region.

There have been few published studies on North American tropical biomes for the past decade that can be cited to better understand interannual NPP variations. Notably, a study by Zou et al. (2021) of drought impacts of vegetation conditions in a dry tropical forest at Chamela-Cuixmala Biosphere Reserve (CCBR) on the Pacific coast of Jalisco in southern Mexico found that higher SST anomalies across multiple phases of El Niño events of

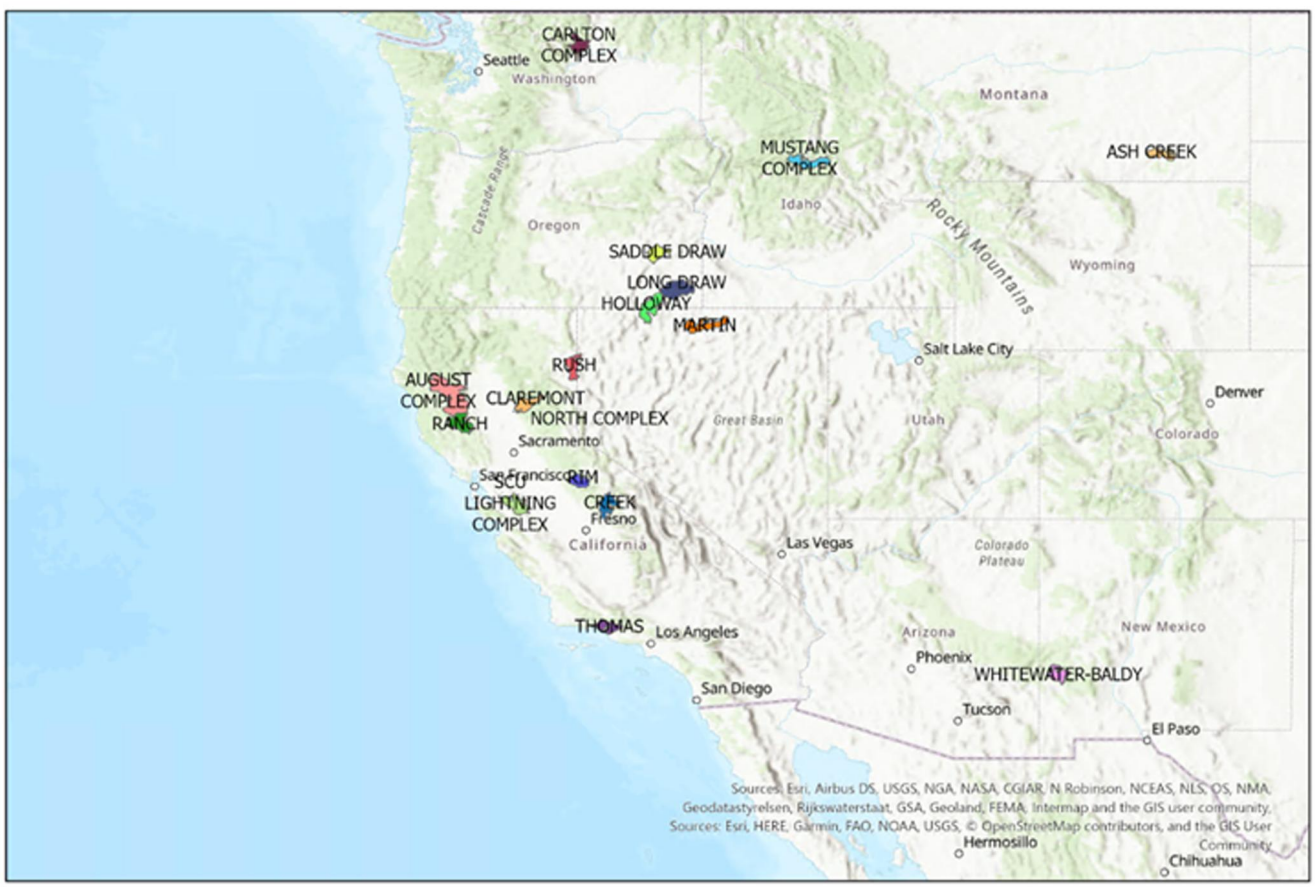


**Figure 8.** Map of the largest fires from 2012 to 2022 in the Western United States.

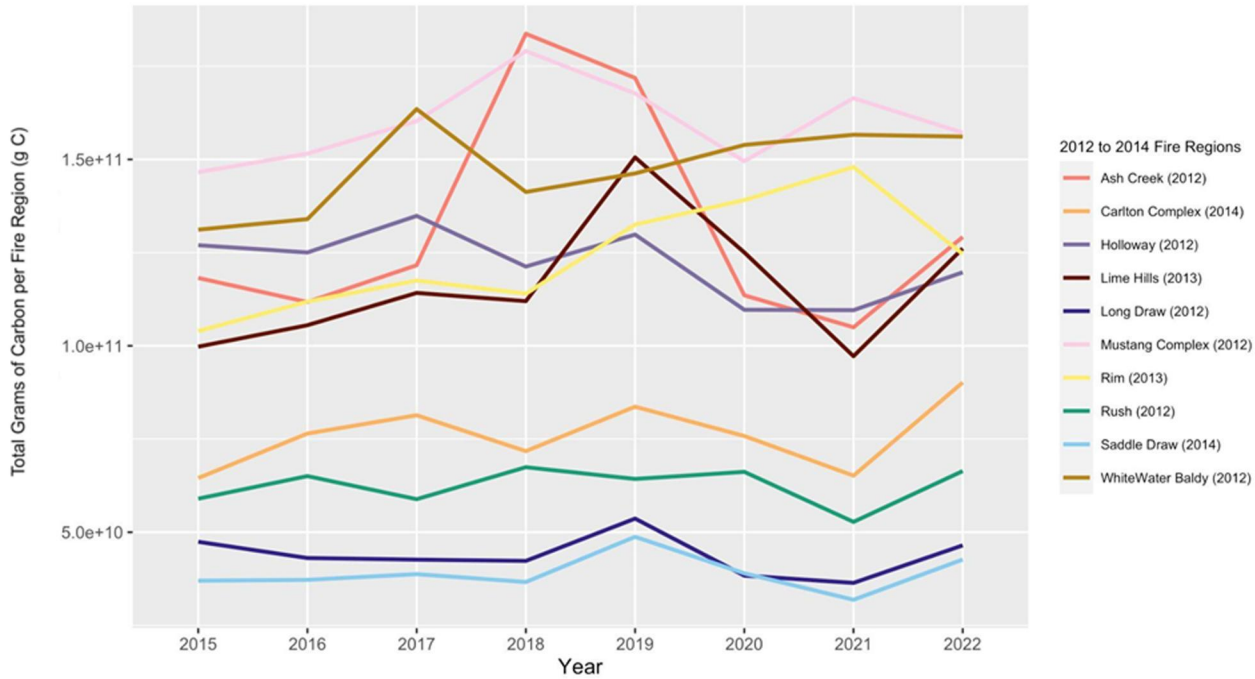


**Figure 9.** Comparison of NPP values in the largest wildfire areas in the United States from 2012 to 2014.

the past 20 years were associated with anomalously high precipitation events in this biome of North America. The greenness state of the forest canopy in this region was sensitive to such precipitation variations, but it was concluded that forest production in the dry season was not significantly influenced by SST anomalies. This is because remotely sensed drought index values at this site did not respond significantly to the specific precipitation patterns during the El Niño events that occurred between 2000 and 2017. These findings are generally consistent

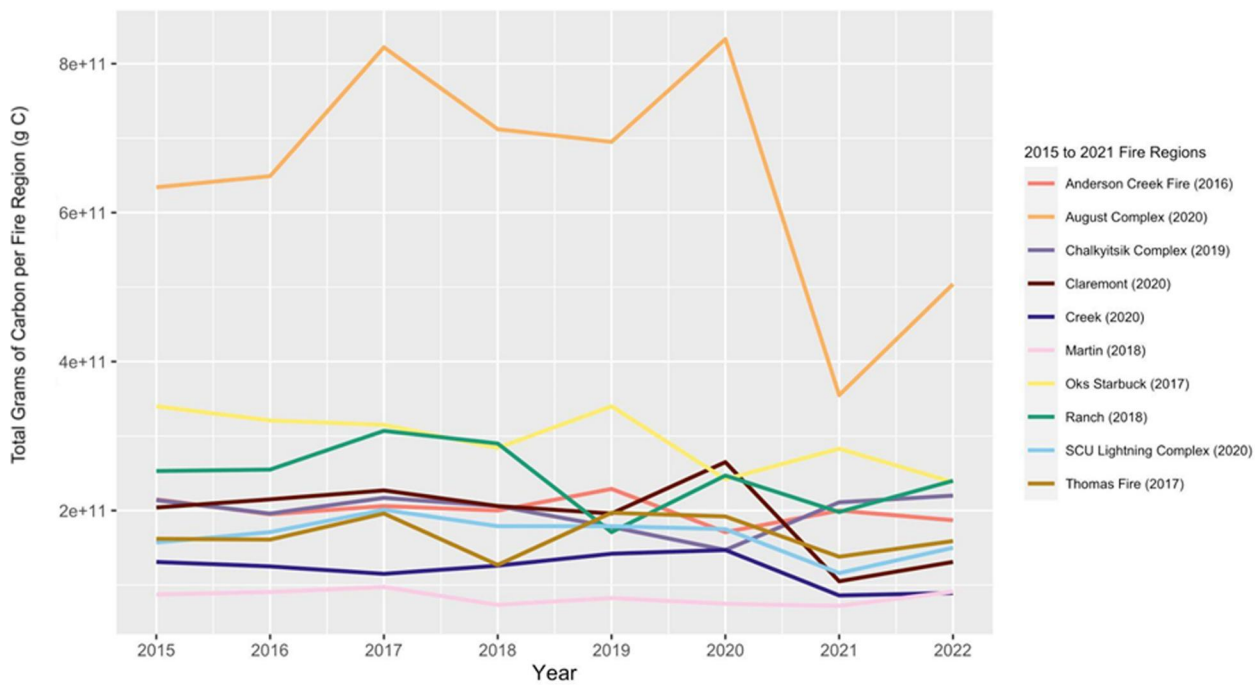


**Figure 10.** Comparison of NPP values in the 10 largest fire burned areas in the United States from 2015 to 2021.

with the CASA model predictions that the total growing season NPP in all tropical and subtropical biomes varied relatively little from 2015 to 2022.

Turning to the CASA model prediction results for NPP recovery in wildfire areas, several large fires that burned in the years 2012–2014 have been studied for early regrowth patterns in the field. For instance, the 2012 Ash Creek wildfire that burned through the Northern Cheyenne Reservation in Montana has been monitored by Donovan et al. (2020), particularly where ponderosa pine (*Pinus ponderosa*) was prevalent before the fire. Tree cover in the burn area declined persistently following wildfire, whereas shrub and annual forb and grass cover increased. Ponderosa pine-dominated ecosystems have been shown to be susceptible to major shifts in ecosystem structure and function following severe wildfire; for example, in the first decade following a mixed-severity fire in western ponderosa systems, live trees experience high mortality and greater snag densities (Roberts et al., 2019). In general, temperate conifer forests dominated by fire-resistant species (species that typically survive low-intensity fires) have been found to experience the lowest relative NPP reductions compared to forests with less fire-resistant species (Sparks et al., 2018).

The Holloway fire of 2012 resulted in a mosaic of burn severity patches throughout the sagebrush-dominated Trout Creek Mountains in Oregon and Nevada. Schuyler et al. (2022) made vegetation community change measurements in the burned area starting in 2013 to evaluate how sage-grouse responded to post-wildfire sagebrush (*Artemisia sp*.) conditions. Mean shrub cover was found to decrease from 25% to 13% from 1-year pre-fire to 1-year post-fire and then gradually increase to 16% at 7 years post-fire. These authors noted that sagebrush communities are intolerant to frequent high-severity burning, and these shrublands take decades to recover due to low precipitation rates and the inability to resprout following fire.

The Carlton Complex lightning fires of 2014 in the Methow Valley, Washington burned through mostly shrub-steppe grasslands and dry conifer forest. In a study of landscape-scale vegetation recovery, Churchill et al. (2022) reported that large patches of high-severity fire in mixed-conifer forest stands homogenized the post-fire landscape patterns towards conditions dominated by non-forest vegetation types. Patches of closed-canopy forest were reduced by this high-severity fire and most open-canopy forest was lost. The older closed-canopy forest that did not burn completely was located on drier locations where future climate projections indicate high drought vulnerability and risk of high-severity fire.

To put the CASA model prediction of post-fire recovery into a broader context, a data set of post-fire conifer regeneration from 10,230 field plots in the western region of the United States was compiled by Davis et al. (2023). These authors reported that warmer, drier climate conditions are leading to lower tree regeneration after wildfires in the past decade, compared to the decades of the 1980s and 1990s. The study quantified the importance of fire-caused tree mortality, which limits seeds available for tree regeneration during warming, drying climate conditions. Lower elevation tree species (e.g., *Pinus ponderosa*) have already experienced a significant decline in recruitment probability between the 1981 to 2000 and the 2001 to 2020 time periods, while higher elevation species such as *P. contorta* and *P. engelmannii* were predicted to experience more declines in the coming decades following wildfires.

## 5. Conclusions

CASA model predictions from 2015 to 2022 showed variations between high and low periods in growing season NPP totals in most biomes of North America. Rapid declines in total biome NPP from 2019 to 2020–2021 were estimated for all biomes except those in the tropical forest zones. In contrast to the climate patterns in the temperate biomes that developed into severe widespread drought in 2020 and 2021 due to drought, growing season NPP in the tundra biome was depressed in these same years by colder temperature induced drought conditions at the high latitudes of North America. Drought severity indicators were closely associated with declines of different magnitudes in NPP in most biomes. Trends in NPP in areas of some of the largest wildfires in North America that burned between 2012 and 2014 indicated that extreme drought periods can depress NPP recovery even 5–7 years post-fire. Explanations from recent field studies in these burned areas imply that regenerating tree cover has declined following wildfires in the western United States. Inversely, annual forb and grass cover has increased and is relatively more susceptible to extreme drought than were the pre-fire forests and woodlands.

## Data Availability Statement

The CASA model source code used in this study and CASA model NPP output geotiff files are all available for download at the NASA-CASA Github repository in version 2024, openly accessible at https://zenodo.org/records/10525125 (Potter & Pass, 2023, https://doi.org/10.5281/zenodo.10525125). There are no access limitations nor licensing conditions for the use of this software.

**Acknowledgments**
The authors thank Jessica McCarty for thoughtful reviews of the manuscript and valuable advice related to wildfire impacts on ecosystems.

## References

Amthor, J. S., Chen, J. M., Clein, J. S., Frolking, S. E., Goulden, M. L., Grant, R. F., et al. (2001). Boreal forest $CO_2$ exchange and evapotranspiration predicted by nine ecosystem process models: Intermodel comparisons and relationships to field measurements. *Journal of Geophysical Research*, *106*(D24), 33623–33648. https://doi.org/10.1029/2000jd900850

Behrenfeld, M. J., Randerson, J. T., McClain, C. R., Feldma, G. C., Los, S. Q., Tucker, C. I., et al. (2001). Biospheric primary production during an ENSO transition. *Science*, *291*(5513), 2594–2597. https://doi.org/10.1126/science.1055071

Berner, L. T., Law, B. E., & Hudiburg, T. W. (2017). Water availability limits tree productivity, carbon stocks, and carbon residence time in mature forests across the western US, Biogeosciences. *Biogeosciences*, *14*(2), 365–378. https://doi.org/10.5194/bg-14-365-2017

Berner, L. T., Massey, R., Jantz, P., Forbes, B. C., Macias-Fauria, M., Myers-Smith, I., et al. (2020). Summer warming explains widespread but not uniform greening in the Arctic tundra biome. *Nature Communications*, *11*(1), 4621. https://doi.org/10.1038/s41467-020-18479-5

Bonan, G. B. (1989). A computer model of the solar radiation, soil moisture and soil thermal regimes in boreal forests. *Ecological Modelling*, *45*(4), 275–306. https://doi.org/10.1016/0304-3800(89)90076-8

Bonney, M. T., Danby, R. K., & Treitz, P. M. (2018). Landscape variability of vegetation change across the forest to tundra transition of central Canada. *Remote Sensing of Environment*, *217*, 18–29. https://doi.org/10.1016/j.rse.2018.08.002

Churchill, D., Jeronimo, S. M. A., Hessburg, P. F., Cansler, C. A., Povak, N. A., Kane, V. R., et al. (2022). Post-fire landscape evaluations in Eastern Washington, USA: Assessing the work of contemporary wildfires. *Forest Ecology and Management*, *504*, 119796. https://doi.org/10.1016/j.foreco.2021.119796

Davis, K. T., Robles, M. D., Kemp, K. B., Higuera, P. E., Chapman, T., Metlen, K. L., et al. (2023). Reduced fire severity offers near-term buffer to climate-driven declines in conifer resilience across the western United States. *Proceedings of the National Academy of Sciences of the United States of America*, *120*(11). https://doi.org/10.1073/pnas.2208120120

Didan, K. (2015). MOD13C1 MODIS/terra vegetation indices 16-day L3 global 0.05Deg CMG V006 [Dataset]. *NASA EOSDIS Land Processes DAAC*. https://doi.org/10.5067/MODIS/MOD13C1.006

Donovan, V. M., Twidwell, D., Uden, D. R., Tadesse, T., Wardlow, B. D., Bielski, C. H., et al. (2020). Resilience to large, "catastrophic" wildfires in North America's grassland biome. *Earth's Future*, *8*(7), e2020EF001487. https://doi.org/10.1029/2020ef001487

Eidenshink, J., Schwind, B., Brewer, K., Zhu, Z., Quayle, B., & Howard, S. (2007). A project for monitoring trends in burn severity. *Fire Ecology*, *3*(1), 3–21. https://doi.org/10.4996/fireecology.0301003

Friedl, M. A., McIver, D., Hodges, J., Zhang, X., Muchoney, D., Strahler, A., et al. (2002). Global land cover mapping from MODIS: Algorithms and early results. *Remote Sensing of Environment*, *83*(1–2), 287–302. https://doi.org/10.1016/s0034-4257(02)00078-0

Hicke, J. A., Asner, G. P., Randerson, J. T., Tucker, C. J., Los, S. O., Birdsey, R., et al. (2002). Satellite-derived increases in net primary productivity across North America, 1982-1998. *Geophysical Research Letters*, *29*(10), 1427. https://doi.org/10.1029/2001gl013578

Hijmans, R. (2023). Geographic data analysis and modeling. *R package version*, *3*, 6–14. Retrieved from https://CRAN.R-project.org/package=raster

Hsiang, S., Kopp, R. E., Jina, A., Rising, J., Delgado, M., Mohan, S., et al. (2017). Estimating economic damage from climate change in the United States. *Science*, *356*(6345), 1362–1369. https://doi.org/10.1126/science.aal4369

Jay, S., Potter, C., Crabtree, R., Genovese, V., Weiss, D., & Kraft, M. (2016). Evaluation of modelled net primary production using MODIS and Landsat satellite data fusion. *Carbon Balance and Management*, *11*(1), 8. https://doi.org/10.1186/s13021-016-0049-6

Jumikis, A. R. (1966). *Thermal soil mechanics*. Rutgers University Press.

Kanamitsu, M., Ebisuzaki, W., Woollen, J., Yang, S.-K., Hnilo, J. J., Fiorino, M., & Potter, G. L. (2002). NCEP–DOE AMIP-II Reanalysis (R-2). *Bulletin of the American Meteorological Society*, *83*(11), 1631–1643. https://doi.org/10.1175/bams-83-11-1631(2002)083<1631:nar>2.3.co;2

Liang, X., Hui, F., Tanaka, E., & Seimon, D. (2021). ggmatplot: A quick and easy way of plotting the columns of two matrices or data frames against each other using ggplot2.

Malmstrom, C. M., Thompson, M. V., Juday, G. P., Los, S. O., Randerson, J. T., & Field, C. B. (1997). Interannual variation in global scale net primary production: Testing model estimates. *Global Biogeochemical Cycles*, *11*(3), 367–392. https://doi.org/10.1029/97gb01419

Mariën, B., Dox, I., De Boeck, H. J., Willems, P., Leys, S., Papadimitriou, D., & Campioli, M. (2021). Does drought advance the onset of autumn leaf senescence in temperate deciduous forest trees? *Biogeosciences*, *18*(11), 3309–3330. https://doi.org/10.5194/bg-18-3309-2021

Monteith, J. L. (1972). Solar radiation and productivity in tropical ecosystems. *Journal of Applied Ecology*, *9*(3), 747–766. https://doi.org/10.2307/2401901

NOAA National Centers for Environmental Information (NCEI). (2023). U.S. Billion-dollar weather and climate disasters. https://doi.org/10.25921/stkw-7w73

Olson, D. M., Dinerstein, E., Wikramanayake, E. D., Burgess, N. D., Powell, G. V. N., Underwood, E. C., et al. (2001). Terrestrial ecoregions of the world: A new map of life on Earth. *BioScience*, *51*(11), 933–938. https://doi.org/10.1641/0006-3568(2001)051[0933:teotwa]2.0.co;2

Philip, S., Johnson, M. S., Potter, C., Genovesse, V., Baker, D. F., Haynes, K. D., et al. (2019). Prior biosphere model impact on global terrestrial $CO_2$ fluxes estimated from OCO-2 retrievals. *Atmospheric Chemistry and Physics*, *19*(20), 13267–13287. https://doi.org/10.5194/acp-19-13267-2019

Potter, C., Klooster, S., Genovese, V., Hiatt, C., Boriah, S., Kumar, V., et al. (2012). Terrestrial ecosystem carbon fluxes predicted from MODIS satellite data and large-scale disturbance modeling. *International Journal of Geosciences*, *03*(03), 469–479. https://doi.org/10.4236/ijg.2012

Potter, C., Klooster, S., Myneni, R., Genovese, V., Tan, P., & Kumar, V. (2003). Continental scale comparisons of terrestrial carbon sinks estimated from satellite data and ecosystem modeling 1982–1998. *Global and Planetary Change*, *39*(3–4), 201–213. https://doi.org/10.1016/j.gloplacha.2003.07.001

Potter, C., & Pass, S. (2023). CASA model source code, release (version 2023.1.0) [Software]. *NASA*. Retrieved from https://github.com/SPass-space/NASA-CASA/

Potter, C., Randerson, J., Field, C., Matson, P., Vitousek, P., Mooney, H., & Klooster, S. (1993). Terrestrial ecosystem production: A process model based on global satellite and surface data. *Global Biogeochemical Cycling*, *7*(4), 811–841. https://doi.org/10.1029/93gb02725

Potter, C. S., Klooster, S. A., & Brooks, V. (1999). Interannual variability in terrestrial net primary production: Exploration of trends and controls on regional to global scales. *Ecosystems*, *2*(1), 36–48. https://doi.org/10.1007/s100219900056

Potter, C. S., Wang, S., Nikolov, N. T., McGuire, A. D., Liu, J., King, A. W., et al. (2001). Comparison of boreal ecosystem model sensitivity to variability in climate and forest site parameters. *Journal of Geophysical Research*, *106*(33), 33671–33687. https://doi.org/10.1029/2000jd000224

Priestley, C. H. B., & Taylor, R. J. (1972). On the assessment of surface heat flux and evaporation using large-scale parameters. *Monthly Weather Review*, *100*(2), 81–92. https://doi.org/10.1175/1520-0493(1972)100<0081:otaosh>2.3.co;2

Public Policy Institute of California. (2022). Policy brief: Drought and California's agriculture. Retrieved from www.ppic.org/publication/policy-brief-drought-and-californias-agriculture

Randerson, J. T., van der Werf, G. R., Giglio, L., Collatz, G. J., & Kasibhatla, P. S. (2018). *Global fire emissions database, version 4.1 (GFEDv4)*. ORNL DAAC. https://doi.org/10.3334/ORNLDAAC/1293

R Core Team. (2022). *R: A language and environment for statistical computing*. R Foundation for Statistical Computing. Retrieved from https://www.R-project.org/

Roberts, C. P., Donovan, V. M., Wonkka, C. L., Powell, L. A., Allen, C. R., Angeler, D. G., et al. (2019). Fire legacies in eastern ponderosa pine forests. *Ecology and Evolution*, *9*(4), 1869–1879. https://doi.org/10.1002/ece3.4879

Schuyler, E., Hagen, C., Anthony, C., Foster, L., & Dugger, K. (2022). Temporal mismatch in space use by a sagebrush obligate species after large-scale wildfire. *Ecosphere*, *13*(9). https://doi.org/10.1002/ecs2.4179

Smith, A. (2022). 2021 U.S. billion-dollar weather and climate disasters in historical context. Technical Report. Retrieved from www.ncdc.noaa.gov/billions

Sparks, A. M., Kolden, C., Smith, A., Boschetti, L., Johnson, D., & Cochrane, M. (2018). Fire intensity impacts on post-fire response of temperate coniferous forest net primary productivity. *Biogeosciences*, *15*(4), 1173–1183. https://doi.org/10.5194/bg-15-1173-2018

Statistics Canada. (2021). Production of principal field crops. Retrieved from https://www150.statcan.gc.ca/n1/daily-quotidien/211203/dq211203b-eng.htm

Stockdale, T., Balmaseda, M., & Ferrant, L. (2017). The 2015/2016 El Niño and beyond. *ECMWF Newsletter*, *151*, 16–21.

Svoboda, M. D., LeComte, D., Hayes, M. J., Heim, R., Gleason, K. L., Angel, J. R., et al. (2002). The drought monitor. *Bulletin of the American Meteorological Society*, *83*(8), 1181–1190. https://doi.org/10.1175/1520-0477-83.8.1181

Umphlett, N. A., Woloszyn, M., Parker, B. A., Akyuz, F. A., Bergantino, A. R., Brotherson, S., et al. (2022). *The 2020–2021 drought in the U.S. Northern Plains and Canadian Prairies: Initial assessment of impacts and response to build resilience during an ongoing drought*. NOAA National Integrated Drought Information System.

Wickham, H. (2016). *ggplot2: Elegant graphics for data analysis*. Springer-Verlag.

Zou, L., Cao, S., Zhu, Z., & Sanchez-Azofeifa, A. (2021). Assessment of the response of tropical dry forests to El Nino southern oscillation. *Ecological Indicators*, *133*, 108390. https://doi.org/10.1016/j.ecolind.2021.108390